JCTC Journal of Chemical Theory and Computation

ARTICLE

pubs.acs.org/JCTC

Solvent Effects on the Radiative and Nonradiative Decay of a Model of the Rhodopsin Chromophore

Aurora Muñoz-Losa,* M. Elena Martín, Ignacio Fdez. Galván, M. Luz Sánchez, and Manuel A. Aguilar

Química Física, Universidad de Extremadura, Avda. de Elvas s/n 06071 Badajoz, Spain

Supporting Information

ABSTRACT: The radiative and nonradiative decay of a model with five double bonds of the 11-*cis*-retinal protonated Schiff base was studied both in vacuum and in methanol solution using an extended version of the averaged solvent electrostatic potential from molecular dynamics data (ASEP/MD) method that allows the location of crossing points between free energy surfaces both in equilibrium and in frozen solvent conditions. The multireference quantum method CASSCF was used for the description of the states of interest, while the solvent structure was obtained from molecular dynamics simulations. Electron dynamic correlation corrections to the energy were included at CASPT2 level. Unlike in gas phase, where only two states seem to be implicated, in methanol solution, three states are necessary to describe the photoisomerization process. At the Franck−Condon point the S_1 and S_2 states are almost degenerate; consequently, the S_1 surface has a region with an ionic character (^1B_u-like) and another one with a covalent character (^2A_g-like). Emission from the ionic minima is responsible for the low-frequency part of the fluorescence band, while emission from the covalent minima originates the high-frequency part. The ionic minimum is separated from the conical intersection yielding the all-*trans* isomer by an energy barrier that was estimated in 0.7 kcal/mol. The geometry of the optimized conical intersection was found at a torsion angle of the central double bond close to 90° both in vacuum and in methanol solution. This large torsion in addition to the accompanying charge displacements forces a strong solvent reorganization during the de-excitation process which slows down the photoisomerization kinetics in methanol with respect to the gas phase. Solvent fluctuations modulate the minima depth and the barrier height and could explain the multiexponential relaxation time observed in the experiments.

1. INTRODUCTION

Although the theoretical study of solvent effects on the evolution of molecules in excited states has received an increasing attention in the last years, nonradiative (nonadiabatic) processes have been comparatively less studied than radiative processes (fluorescence or phosphorescence). The reasons are obvious, from the difficulties inherent to the presence of a solvent, as are the existence of a manifold of configurations thermally accessible, to the great number of solvent molecules involved or the interplay between solute and solvent dynamics, one must add the complications associated to the study of nonadiabatic processes,[1−5] processes that imply more than one potential energy surface. It is usual to classify nonadiabatic processes as internal conversion (IC) or intersystem crossing (ISC) depending on the spin symmetry of the states involved. Associated with this nonadiabatic process we find a potential energy surface crossing named conical intersection (CI) or singlet−triplet crossing (STC). Nowadays, there are several techniques and algorithms available that permit the determination of those geometries for which CI and STC appear and also for the minimal energy conical intersection geometries (MECI), which are considered as the most probable radiationless decay sites.

There have been several proposals in the literature to include solvent effects in the study of IC processes. Burghardt et al.,[6,7] for instance, use dielectric continuum methods. These authors introduce an explicit coordinate for the solvent, which permits them to study the solvation dynamics during the internal conversion process. Polarizable continuum models (PCM) have been used by Barone et al. in the study of uracil derivates.[8] Methods that allow a more detailed description of the solvent have also been proposed; so for instance, Yamazaki and Kato[9] use the reference interaction site model self-consistent field (RISM-SCF)[10] method for describing the solvent dynamics during energy surface crossing in ethylene and $CH_2NH_2^+$ in polar solvents. This group has also studied conical intersections in a small protonated Schiff base model of retinal in methanol solution, stressing the importance of the electron correlation in the structural and energetic properties of the MECI.[11] Other groups[12−14] have used quantum mechanics/molecular mechanics (QM/MM) methods to locate CI, generally in frozen solvent conditions, although in some cases the solvent dynamics has been also considered.

In a previous study[15] we developed an extended version of the averaged solvent electrostatic potential from molecular dynamics (ASEP/MD) method that permitted the study of the solvent effects on radiationless decay processes both in equilibrium and nonequilibrium (frozen) solvent conditions. As an application of the method, we studied the photophysics of acrolein in aqueous solution. Because of the small size of acrolein, solvent reorganization was not a necessary condition for the photoisomerization reaction, and the molecule exhibited a similar behavior in solution and in gas phase. In the present study we are interested in the location and characterization of the principal critical points

Received: April 28, 2011
Published: November 04, 2011

ACS Publications © 2011 American Chemical Society

(minima, CI, etc) on the first two low-lying excited states of a model of the rhodopsin chromophore in methanol solution.

Rhodopsin is a protein that is highly specialized in the detection of photons. Its chromophore, retinal, is an A1-vitamin derivative and is formed by a β-ionone ring and a polyene chain bonded covalently through a Schiff bond to the Lys296 residue of the protein. As a consequence of the absorption of one photon, the protonated Schiff base of the 11-*cis*-retinal (PSB11) undergoes a rotation, and it transforms into its all-*trans* isomer in a very fast process that, inside the protein, happens in less than 200 fs.[16,17] The speed of the process and the lack of radiation emission is explained by the existence of a conical intersection between the potential energy surfaces of the first excited state and the ground state. These states are clearly differenced by its charge distribution, that is, the ground state has a predominantly covalent character (dot−dot) with a localized electronic distribution, whereas the excited crossing state has a predominantly ionic character (hole−pair), which means that the charges are delocalized over the molecule. Several studies of this nonadiabatic process have been carried out. Martínez et al.,[12b] for instance, used the floating occupation molecular orbital approach (FOMO) with semiempirical methods to locate the MECI in vacuum, although the energies are not in agreement with those obtained with ab initio calculations. In a previous work[12a] they used a QM/MM method to solvate an analogue of PSB11 with 57 MM water molecules; they found that the stabilization of the MECI with respect to in vacuum conditions is about 7 kcal/mol. Olivucci et al. have largely studied different aspects of this IC, they have analyzed different models of the PSB11 in vacuum,[13,18] the effects of the counterions,[19] and more recently, the effect of the opsin.[13,20] Burghardt et al.[6] use a dielectric continuum model to describe the electrostatic effects of the environment in protonated Schiff bases, like PSB11, concluding that the CI is lost in frozen solvent conditions. Send and Sundholm[21] carried out a time-dependent density functional theory (TD-DFT) study in vacuum and inside the protein; they suggested that the electron excitation produces the torsion of the β-ononic ring, and then the torsion is propagated along the carbon chain to the C_{11}=C_{12} center to allow the photoisomerization. Warshel and Chu[22] analyze the nature of the surface crossing process in bacteriorhodopsin using a hybrid QM/MM method. It is demonstrated that the motion starts with bond vibrations and evolves to a torsional motion and that surface crossing occurs only in the 90° region. More recently, Kato et al. have published a theoretical study of the *cis*−*trans* photoisomerization of a small PSB11 model with only three double bonds in methanol solution.[11] These authors employed analytical gradients for the location of the MECI at multistate-CASPT2 level[23] and the RISM-SCF method[10] to include the solvent effects. In this study the importance of the dynamical correlation in the structural and energetic properties of two possible MECI has been highlighted.

In a more experimental vein, several authors[24−27] analyzed the photoisomerization process inside the protein, and evidence for the involvement of a conical intersection was obtained. In a recent study, Zgrablić et al.[28] have obtained femtosecond fluorescence spectra of the all-*trans* retinal Schiff base in several polar and apolar solvents. The analysis of the time-resolved fluorescence spectrum in methanol reveals a complex spectral behavior that could be originated by emissions from different structures and states. Other experimental data to account for is that, in methanol, the photoisomerization is 2 orders of magnitude slower than in the protein, while calculations in gas phase report a process as fast as in protein.[29] Elucidating if this slow reaction in methanol is due to changes in the free energy surfaces of the states involved in the photoisomerization or if, on the contrary, it is related to solvent dynamics is one of the aims of this paper. It is worth noting that during the *cis*−*trans* photoisomerization of retinal, there are parts of the solute molecule that can suffer large displacements, consequently, it can be expected that, in opposition to what was found in acrolein, the solvent reorganization would become an important step in the reaction mechanism and lead to large differences between the gas phase and in solution behavior. A second aim is the location of the possible minima that could explain the fluorescence spectrum of the chromophore in methanol. In short, we expect to clarify the role that the solvent plays in the radiative and nonradiative decay processes.

The rest of the paper is organized as follows: In Section 2 the main features of the method will be explained, and the computational aspects will be detailed. In Section 3 the in vacuum and in methanol solution results will be discussed, and finally, the main conclusions will be reported in Section 4.

2. METHODS AND DETAILS

ASEP/MD is a QM/MM effective Hamiltonian method that makes use of the mean field approximation.[30] The method combines QM and MD techniques with the particularity that full QM and MD calculations are alternated and not simultaneous. During the MD simulations, the intramolecular geometries and charge distributions of all molecules are considered as fixed, and the interaction is calculated with MM. From the resulting data, the average electrostatic potential generated by the solvent on the solute can be obtained. This potential is introduced as a perturbation into the solute's quantum mechanical Hamiltonian, and by solving the associated Schrödinger equation, a new charge distribution for the solute is obtained, which is used in the next MD simulation. The iterative process is repeated until the electron charge distribution of the solute and the solvent structure around it become mutually equilibrated.

To locate a optimized conical intersection between two electronic states, we combine the ASEP/MD method with an algorithm due to Bearpark et al.[31] The algorithm simultaneously minimizes the in solution energy difference between the two intersecting states and the energy of the crossing seam between the two potential energy surfaces. Details of the method can be found elsewhere.[15]

We consider two possible regimes for the solvent depending on whether it is in an equilibrium or nonequilibrium (frozen) situation with the solute. In the former case, the solvent is equilibrated at every point with the solute charge distribution of the adiabatic state on which the initial dynamics takes place, i.e., the S_1 state with ionic character when an S_1/S_0 CI is searched for. Although in the neighborhood of the CI, the S_0 and S_1 states are swapping, the solvent is always in equilibrium with the state of larger ionic character, which is identified by its charge distribution. In the second regime, a frozen solvent structure, which is in equilibrium with the charge distribution of a previous solute structure, is used. In this situation the solvent does not respond to changes in the solute charge distribution. Both situations are extreme cases, the real behavior of the system is expected to be somewhere between them. It is worth noting that the minimum energy conical intersection located in these conditions is an upper limit to the real MECI; in consequence, we do not obtain the absolute MECI but the lowest energy CI subject to the condition that the solvent is either in equilibrium with the S_1 state

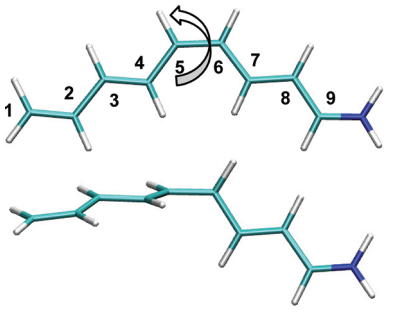

Figure 1. Planar M1 and twisted EQ-MECI M1 pictures and numbering of the carbon skeleton.

or frozen. Therefore from now on we call this optimized conical intersection in solution as EQ-MECI in equilibrium and FS-MECI with frozen solvent.

Once the geometries of interest (ground- and excited-state minima, EQ-MECI, etc.) have been located the free energy differences, ΔG, between them are calculated as sums of two terms

$$\Delta G = \Delta E_{QM} + \Delta G_{int} \quad (1)$$

where ΔE_{QM} is the difference in the internal quantum energy of the solute between the two geometries and ΔG_{int} is the difference in the solute−solvent interaction energy, which is calculated classically using the free energy perturbation method.[32] In turn, the ΔG_{int} term can be split into two terms $\Delta G_{int} = \Delta E_{int} + \Delta G_{solv}$. The term ΔE_{int} accounts for the difference in the solute−solvent interaction energy between the final and initial state. The last term, ΔG_{solv}, provides the solvent distortion energy, i.e., the energy spent in changing the solvent structure from the initial to the final state.

2.1. Computational Details. The current study tackles the comparison of the excited potential energy surfaces of a model of the 11-*cis*-retinal protonated Schiff base molecule formed by five double bonds in vacuum and in methanol solution. In previous papers[33] it was shown that this model, called M1 (see Figure 1), is adequate in studying the photophysical behavior of the real molecule since it reproduces some of the main features of the experimental absorption spectra:[34] two well separated excited states in vacuum that become almost degenerate in methanol solution. The ground and excited states were described using state-average complete active space self-consistent field (SA-CASSCF) of the first three roots with equal weights. All electrons of the π skeleton were included in the active space, which was spanned by all the configurations arising from 10 valence π electrons in 10 orbitals (10e, 10o). The split-valence 6-31G(d) basis set was employed. It is well-known that to obtain an accurate description of the energetic properties of photoexcited systems, the dynamic electronic correlation must be included. In our case, we used the second-order perturbation method CASPT2. Since analytical gradients are not available for this method in the MOLCAS program, carrying out CASPT2 geometry optimizations was impractical, and therefore we only recalculated the electronic energies with CASPT2 at the geometries located with SA-CASSCF. In the case of the MECI, also multistate CASPT2[23] calculations were performed. All the calculations were performed with a development version of the ASEP/MD program using the data provided by Gaussian98[35] and Moldy.[36] The dynamical correlation corrections were calculated with MOLCAS 6.4.[37] Calculations were performed with no ionization potential electron affinity (IPEA) shift[38] to be consistent with previous calculations done with older MOLCAS versions. An additional imaginary shift of 0.1i E_h was included in order to minimize the appearance of intruder states. All the minima, both in vacuum and in methanol solution, were confirmed by analytical Hessian calculations at CASSCF with a harmonic approximation and, in the case of in methanol minima, supposing that the solvent remains frozen during the solute vibration.

To locate the CI points, we used a quasi-Newton method where the approximate Hessian was updated by using the Broyden−Fletcher−Goldfarb−Shanno (BFGS) algorithm.

A total of 331 molecules were simulated with fixed intramolecular geometry by combining Lennard-Jones interatomic interactions with electrostatic interactions. The solvent was represented by 330 molecules of methanol using AMBER nonbonded parameters[39] in a cubic box of 28.2 Å side (test calculations performed with 1000 methanol molecules did not show significant changes). Also AMBER nonbonded parameters[39] were used for the solute. No counterion was included. Previous studies of Rajamani and Gao[40] and Röhrig et al.[41] using chloride as counterion find that, because of the large dielectric screening effect of methanol, the effect of the counterion on the structure and spectrum of the solute is minimal. This has been corroborated by experiments showing that the position of the chromophore absorption band in polar solvents is not affected by the nature of the counterion.[42] Periodic boundary conditions were applied, and spherical cutoffs were used to truncate the molecular interactions at 9.0 Å. A time step of 0.5 fs was used. The electrostatic interaction was calculated with the Ewald method. The temperature was fixed at 298 K by using a Nosé−Hoover thermostat. Each MD calculation simulation was run for 75 ps (25 ps equilibration, 50 ps production). In solution, the results are affected by statistical uncertainty due to the finite size of the MD sampling, and we take average values of the last five ASEP/MD cycles. Given that 10−15 total cycles are performed, the effective times are around 400−750 ps for equilibration and 250 ps for production.

3. RESULTS AND DISCUSSION

In previous papers[32] it was shown that the solvent modifies the relative stability of the low-lying excited states of the 11-*cis*-retinal protonated Schiff base and of several molecules used as models of the rhodopsin chromophore, M1 among them. In gas phase the absorption spectrum displays two bands separated by almost 1 eV, corresponding to transitions from the ground state (covalent or ^2A_g-like in character) to the first excited state, which has ionic character (^1B_u-like) and to the second excited state, with a covalent character. The transition to the covalent excited state is generally associated to a smaller oscillator strength and can be difficult to detect experimentally in some cases. In methanol solution a single band is observed in the absorption spectrum.

In the next two subsections we will describe the main characteristics of the two low-lying excited states of M1 both in gas phase (Section 3.1) and in methanol solution (Section 3.2). We will show that in both phases, it has been possible to locate several local minima on S_1. We will also discuss the solvent effects on the relative stability of the EQ-MECI. A priori, any double bond of the 11-*cis*-retinal molecule could undergo photoisomerization; in fact, in solution, conical intersections have been identified[12b] that lead to the all-*trans* retinal and to several di-*cis*

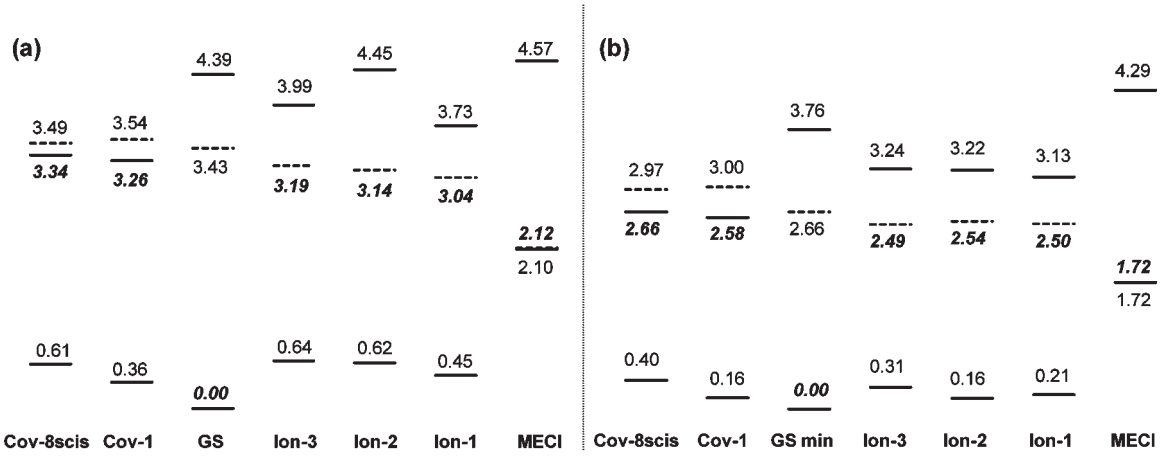

Figure 2. Relative energies (in eV) with respect to the in equilibrium ground state at CASSCF level (a) and at CASPT2//CASSCF level (b) in vacuum for the GS, Ion-1, Ion-2, Ion-3, Cov-1, and Cov-8scis minima, and the MECI. Covalent states are in solid lines, and ionic states are in dashed lines. In bold and italic, the optimized state energies.

isomers. The process is more selective inside the rhodopsin pocket where the only bond that undergoes the rotation is the central double bond C_{11}=C_{12}. The final product in this case is the all-*trans* retinal. It has been suggested[19,43] that the presence of a counterion from the protein can favor the isomerization of this particular bond. In our study we mainly focus on the photoisomerization of the central double bond, although other possibilities are commented.

3.1. In Gas Phase. Figure 2 displays the gas phase transition energies computed at CASSCF and CASPT2 levels. For all the structures considered (FC, minima, MECI), the ionic excited state is more stable than the excited covalent state, except in the covalent-state minima. So, for instance, in the FC point the first two excited states are very well-defined and separated, about 1 eV independently of the calculation level, CASSCF or CASPT2, used. The same is valid in the MECI region. As has been suggested in previous studies[18b] and our calculations confirm, the covalent excited state is not directly involved in the conical intersection associated to the internal conversion process in vacuum. Only two states, ground and ionic, are involved in the photoisomerization reaction. The main structural parameters of the minima located in gas phase are gathered in Table 1. At the beginning of the absorption process, the molecule has the planar structure of the ground state with a clear alternation of single and double bond lengths. Thus, the bond length alternation (BLA), that is, the difference between the length of formal simple and double bonds, is 0.39 Å. The main characteristic of the potential energy surface of the ionic excited state is the presence of several local minima and of a CI. The minima were located at 2.50, 2.54, and 2.49 eV with respect to the ground-state minimum at CASPT2//CASSCF level and only around 0.15 eV under the FC point. These minima, called from now on Ion-1, Ion-2, and Ion-3, respectively, are very close in energy, and all of them display a planar structure. The Ion-1 minimum has a single- and double-bond distribution opposite to that displayed by the ground state: the BLA value is −0.14 Å (the minus sign indicates the interchange in the nature of single and double bonds). In the Ion-2 minimum all the central bonds have the same length, and consequently, the BLA value is 0.00 Å. Finally, the Ion-3 minimum displays a large bond alternation which translates in a BLA value of −0.24 Å. It is worth noting that the three ionic minima differ from each other in less than 1.0 kcal/mol. The three structures are local minima confirmed through frequency calculations, and we found several low-frequency modes corresponding to movements in the molecular plane, indicating that the surface between the minima is relatively flat. The presence of these many minima could be an artifact of using CASSCF method in the optimization. In fact, a previous study by Valsson and Filippi,[44] several minima were found at CASSCF level, whereas a single one was found with other methods that include dynamical correlation. The minimal energy CI is placed at a dihedral angle $C_4C_5C_6C_7$ twist of 90° with an energy that is 1.72 eV above the ground-state minimum, i.e., the MECI is almost 0.80 eV more stable than the ionic minima and 0.94 eV lower than the FC point. This MECI was confirmed by the MS-CASPT2 method with an energy above the ground-state minimum of 1.73 eV. We find that the ionic minima are separated from the MECI by a very small barrier with a height lower than 1 kcal/mol. The barrier height was estimated through a linear interpolation in internal coordinates between the geometries of the ionic S_1 minimum and MECI, and the obtained value can only be considered as an upper limit, subject to all the approximations of the calculation. In these conditions one expects that most of M1 molecules decay though the CI, consequently a low value of the fluorescence quantum yield is expected.

Table 1. Bond Lengths (in Å) for Ground and the Different Minima of the Excited States and the MECI Points in Vacuo

	GS	Ion-1	Ion-2	Ion-3	Cov-1	MECI
C_1C_2	1.35	1.37	1.36	1.37	1.42	1.36
C_2C_3	1.46	1.42	1.41	1.40	1.38	1.42
C_3C_4	1.35	1.42	1.42	1.43	1.42	1.41
C_4C_5	1.45	1.38	1.41	1.36	1.40	1.38
C_5C_6	1.36	1.46	1.42	1.48	1.42	1.47
C_6C_7	1.45	1.37	1.41	1.36	1.40	1.37
C_7C_8	1.35	1.44	1.42	1.46	1.41	1.42
C_8C_9	1.44	1.38	1.39	1.38	1.41	1.39
C_9N	1.28	1.33	1.33	1.34	1.32	1.32

The MECI geometry is characterized by the great torsion of the $C_4C_5C_6C_7$ dihedral angle and by the increase of the central double-bond length C_5C_6 up to 1.47 Å, 0.11 Å larger than at the ground-state minimum geometry. The rest of the molecule remains planar even when we start the optimization from distorted geometries. The loss of the π character of the C_5C_6 central bond easies its torsion and permits the rotation of the molecule. During the evolution of the system from the FC point to the MECI, the differences between double- and single-bond distances decrease, and the BLA in the MECI becomes −0.10 Å, which has been described in previous works.[45] Other mechanisms for the isomerization are possible, and in particular, a bicycle-pedal mechanism has been proposed to occur inside the protein cavity, where spatial constraints are severe,[46] and it has also been observed in ab initio trajectories in gas phase.[47] We tried to locate other MECI points corresponding to different isomerization mechanisms, including the bicycle-pedal, but the search was not successful in this system.

We also found a planar minimum, named Cov-1, on the covalent excited state. All the bonds display similar bond lengths, consequently the BLA value is very small, only −0.08 Å. This minimum (see Figure 2) is only 0.09 eV above the ionic state minimum. Other minima with energies similar to Cov-1 were found on the covalent excited state by rotation around single bonds, one of these minima denoted as Cov-8scis is also displayed in Figure 2.

From the above results we can conclude that most molecules decay without radiation emission through the CI that connects the ionic and the ground state. The possible fluorescence signal would originate mainly at the ionic state minima, while the contribution of the covalent excited state would be minor, owing to the value of the oscillator strength, which is between 1.0 and 1.6 for the ionic minima and only 0.04 for the covalent one. The presence of several minima points to a complex spectral behavior characterized by several relaxation times. The CASPT2 emission energies are 2.29, 2.38, and 2.17 eV for Ion-1, Ion-2 and Ion-3, respectively, that are somewhat lower than the energy obtained at TD-CAM-B3LYP level, 2.46 eV.[48]

A limitation of our study is that the excited states geometries have been optimized at CASSCF level. Recent papers of Valsson et al.[44] and Yamazaki and Kato[9] have highlighted the importance that the inclusion of the dynamic correlation could have on the optimized geometries of excited states. For M1 we found that the CI is kept when the energies are recalculated at CASPT2 level or MS-CASPT2, the energy difference between the two crossing states being lower than 0.1 kcal/mol. This result agrees with that obtained by Valsson et al.,[44] who concluded that the structures calculated at CASSCF and CASPT2 level are similar in the vicinity of the conical intersection. More important differences are expected at the minima geometries, and in this case, it has been shown that CASSCF tends to overestimate the BLA.[15,44] Translating this trend to M1, it is probable that the different ionic state minima located at CASSCF level would have much closer geometries or even collapse in a single minimum at CASPT2 level; in any case, the similarity in CASPT2 energies for Ion-1, Ion-2 and Ion-3 indicates that the CASPT2 surface is still relatively flat, which can still lead to a complex relaxation behavior.

3.2. In Methanol Solution. With the absorption of one photon, rhodopsin undergoes the isomerization of the 11-*cis*-retinal to all-*trans* form in a very fast process that takes less than 200 fs.[16,17] In methanol the isomerization process is 2 orders of magnitude slower, taking 10 ps for the transformation to the all-*trans* isomer.[16] In this case a transient fluorescent state is formed with a 3 ps fluorescence lifetime, whereas inside the protein this state fluoresces only for 50−60 fs.[17,49] In a recent experimental study, Zgrablić et al.[28] disentangle the different spectro-temporal components that make up the fluorescence spectra. In methanol, three spectral components are isolated that Zgrablić et al. interpret as associated to: (1) the vibrationally relaxed S_1 fluorescence, (2) a vibrationally hot S_1 fluorescence, and (3) a higher-lying emission which was assigned to S_2 fluorescence. Trying to relate these experimental data with the characteristics of the free energy surface of the first two excited states and with the solvent response is the goal of this section.

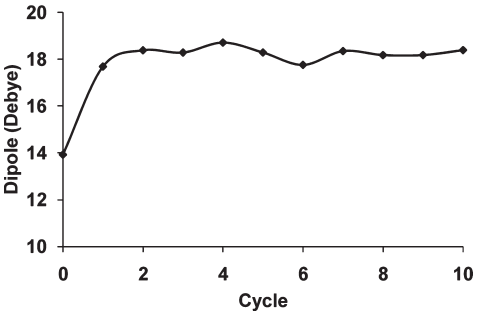

Figure 3. Evolution of the dipole moment in debye during the ground-state optimization vs the number of ASEP/MD cycles employed.

All the states have been optimized in methanol with the ASEP/MD method. The results were obtained as the average of the last five cycles, where the system properties are converged. Figure 3 displays the evolution of the dipole moment during the ASEP/MD procedure. Fluctuations are due to the limited size of the dynamics, as have been analyzed in previous works.[50]

Figure 4 displays the relative stability of the different states of M1 in presence of methanol at CASSCF and CASPT2 level, respectively. All the minima have been obtained in equilibrium solvent conditions and confirmed as such with frequency calculations, while in the Franck−Condon points we have assumed frozen solvent conditions during the transition. Because of its importance in the solvation process, it is interesting to compare the electronic densities of covalent and ionic states, see Figure 5. As a general trend, covalent and ionic excited states are destabilized with respect to the ground state, although not in the same extent. In the ionic state the molecular charge is delocalized along the whole molecule, consequently it is worse solvated than covalent states where the charge is localized in the iminium end. The ionic state destabilization is especially important at the Franck−Condon point at CASPT2 level. We tried to validate this result with MS-CASPT2 calculations, but the resulting off-diagonal terms of the Hamiltonian matrix were too large for the results to be trusted;[51] we enlarged the active space up to 16 orbitals, and this problem was not solved. More details can be found in the Supporting Information. In this situation, where the CASSCF functions are not degenerate and the MS-CASPT2 calculation yields unphysical results, the usual advice is to rely on the single-state CASPT2 energies, and therefore, with appropriate prudence, we take the CASPT2 results at the Franck−Condon point as good. It is worth noting that, as displayed in Figure 4, in methanol, ionic and covalent excited states cross in the neighborhood of the FC point, consequently part of the S_1 surface has an ionic character and part covalent. In order to check the crossing between the two

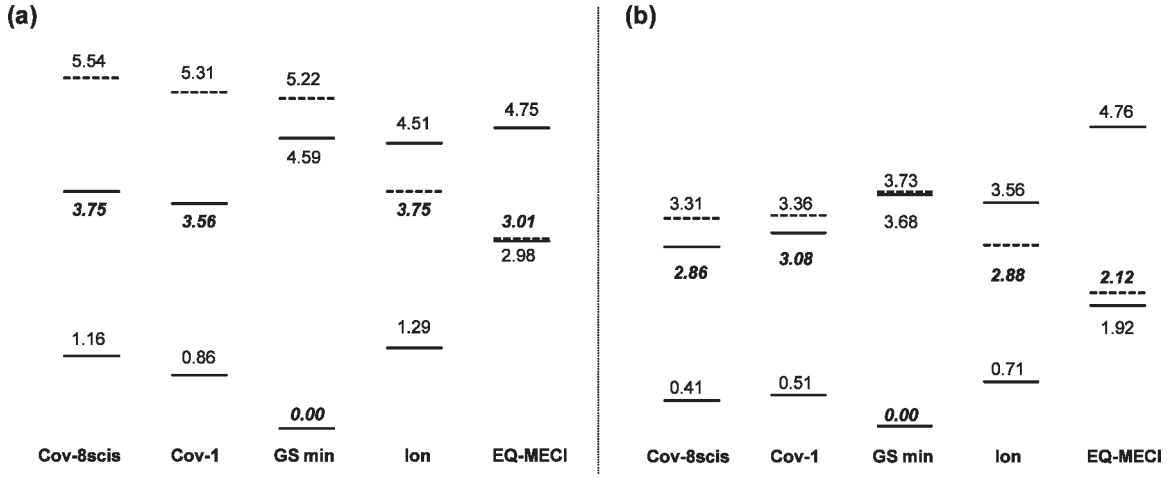

Figure 4. Relative free energies (in eV) with respect to the in equilibrium ground state at CASSCF level (a) and at CASPT2//CASSCF level (b) in methanol for the GS, Ion, Cov-1 and Cov-8scis minima, and the EQ-MECI. Covalent states are in solid lines, and ionic states are in dashed lines. In bold and italic, the optimized state energies.

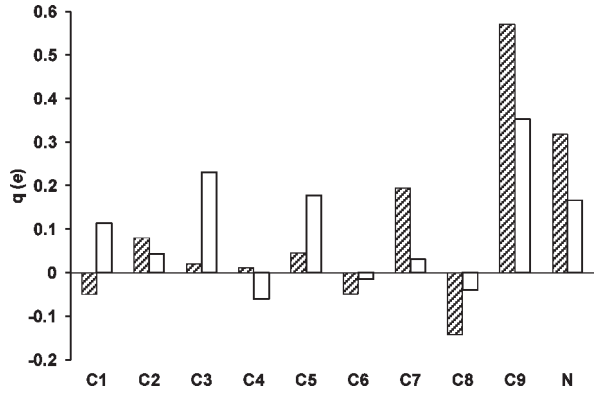

Figure 5. Charges (in *e*, fitted to the CASSCF electrostatic potential) in methanol for the ionic excited state (white columns) and ground state (hatched columns). Charges for the covalent excited state are similar to the ground state.

excited states, 50 configurations were extracted from the molecular dynamics (MD) with the solvent in equilibrium with the ground state, next the electronic transitions were calculated. It was found that the covalent state is below the ionic state in approximately one-half of the configurations. It is observed, too, that the electronic transition to the ionic state remains quasi-invariable, with a fluctuation of 0.02 eV, measured as the standard deviation, whereas the covalent state undergoes larger fluctuations of 0.11 eV.

Regarding the ionic state, a point to remark is that in methanol solution, and independently of the geometry taken as a starting structure (Ion-1, Ion-2, or Ion-3), it was possible to locate only one ionic minimum on S_1 with a relatively flat surface, as in gas phase. This minimum is 0.85 eV under the FC point. The experimental fluorescence energy due to the emission from the ionic excited state is 1.72 eV,[28] whereas our calculated value is 2.17 eV. This last value is almost the same as found in gas phase. The oscillator strength is close to 1. The overestimation of the calculated transition energy is due to: (1) the lower number of conjugated double bonds of M1 (five) with respect to retinal (six) and (2) the nature of the groups bonded to the nitrogen

Table 2. Free Energy Differences and Their Components (in eV) between Pairs of Critical Points at CASSCF Level (in parentheses at CASPT2//CASSCF) in Methanol Solution

	ΔE_{QM}	ΔE_{int}	ΔG_{solv}	ΔG_{int}	ΔG
GS (S_0) → EQ-MECI	2.48	1.75	−1.21	0.54	3.01 (2.12)
GS (S_1) → EQ-MECI	−1.83	0.85	−1.21	−0.37	−2.21 (−1.60)
GS (S_0) → Ion	3.08	1.21	−0.55	0.67	3.75 (2.88)
GS (S_1) → Ion	−1.24	0.31	−0.55	−0.23	−1.47 (−0.87)
GS (S_0) → Cov-1	3.56	−0.11	0.11	0.00	3.56 (3.08)
GS (S_2) → Cov-1	−0.91	−0.23	0.11	−0.12	−1.03 (−0.60)

atom in the iminium group. In M1 the N atom is bonded to two hydrogen atoms, while the experiments have been performed with molecules where the N is bonded to $-CH_3$ or more bulky groups. Consequently, M1 provides larger solvation energy values.[15]

We also found a covalent minimum on S_1 placed 0.60 eV under the FC point and only 0.2 eV over the ionic minimum. The calculated fluorescence emission from this state is 2.57 eV, and the estimated experimental value is 2.17 eV. The deviation from the experimental value, 0.40 eV, is similar to that obtained for the emission from the ionic state and is due to the same reasons. The oscillator strength of the covalent minimum is only 0.08 because at this geometry, S_1 and S_0 have the same character. From a photochemical point of view, the most remarkable characteristic of the ionic excited-state surface is the presence of the S_0/S_1 conical intersection.[5] The EQ-MECI point is placed 0.75 eV under the ionic-state minimum. This value is similar to that found in gas phase. Again, the presence of the EQ-MECI was validated by the MS-CASPT2 method. As the molecule twists, the covalent excited state goes away from the ionic excited state, and at the EQ-MECI, geometry is 2.64 eV above the ionic state. The S_0/S_1 EQ-MECI therefore does not involve the covalent excited state.

Table 2 displays the contributions to the relative free energy differences. The most important contribution is ΔE_{QM}, i.e., the change in the internal energy as a consequence of the solute distortion, that is, changes in the solute geometry and electronic distribution during the photoisomerization. The solvent contribution

Table 3. Bond Lengths (in Å) for the Minima of the Ground and Excited States and the EQ-MECI in Methanol Solution

	GS	Ion	Cov-1	EQ-MECI
C_1C_2	1.34	1.38	1.43	1.36
C_2C_3	1.47	1.40	1.38	1.40
C_3C_4	1.36	1.43	1.44	1.41
C_4C_5	1.45	1.36	1.39	1.36
C_5C_6	1.36	1.49	1.44	1.46
C_6C_7	1.46	1.35	1.38	1.41
C_7C_8	1.36	1.47	1.44	1.39
C_8C_9	1.43	1.38	1.41	1.44
C_9N	1.28	1.33	1.30	1.30

ΔG_{int} is important but only when we compare two states with different charge distributions, the two excited states for instance, but not when the two states have similar charge distribution, ground and covalent excited states. Comparison of ΔE_{QM} with the values displayed in Figure 2 provides the intramolecular contribution to the solvent shift, i.e., the solvent shift due to the change in the solute geometry during the solvation. This contribution is very small in the ionic minimum, 0.11 eV (= 3.19−3.08) and somewhat larger in the covalent minimum, 0.30 eV, and EQ-MECI, 0.35 eV.

Geometrical parameters of the ground- and excited-state minima are gathered in Table 3. In general, the solvent has only a very small effect on the geometry of the different minima. So, for instance, the ground-state geometry is very similar in gas phase, and in methanol, in fact the BLA is the same. The ionic minimum on S_1 is very similar to the Ion-3 gas phase structure with a BLA of −0.28 Å. Similarly to gas phase results, single and double bonds are reverted relative to the ground-state geometry. The S_1 covalent excited-state minimum displays a geometry very similar to the gas phase minimum with only a slight increase of the alternation between single and double bonds providing a BLA value of −0.19 Å. As in gas phase, the minima display planar structures. The solvent effects on the S_0/S_1 EQ-MECI geometry are somewhat larger. As in gas phase, the EQ-MECI structure is characterized by a twisted structure, where the central dihedral angle takes a value of 86°. If we compare the in solution bond lengths with the in vacuum values, one can observe some differences, especially in the iminium end. The rest of the carbon skeleton is hardly affected by the solvent. The BLA in the EQ-MECI geometry is practically zero.

The existence of a stable minimum on S_1 from which the radiative decay is possible points to the existence of a free energy barrier between this minimum and the EQ-MECI. The barrier height was estimated again through a lineal interpolation in internal coordinates between the geometry of the ionic S_1 minimum and the EQ-MECI geometry. Free energy differences were computed every 5° of torsion of the central dihedral. A very small barrier of 0.7 kcal/mol was found with a backbone torsion of 10°. Because of the low height of the barrier, it must be expected that most molecules de-excite through the CI, however, this decay path seems to be less effective in methanol than in gas phase, according to experimental results.[16] In fact, as previously mentioned, theoretical calculations[21] in gas-phase indicate that the de-excitation through the CI is very fast, around 0.1 ps. On the contrary, in methanol it takes about 10 ps.[16] Given that the barrier height and the relative stability of the ionic minimum and the EQ-MECI are completely similar in gas phase and in methanol solution, the differences in the nonradiative

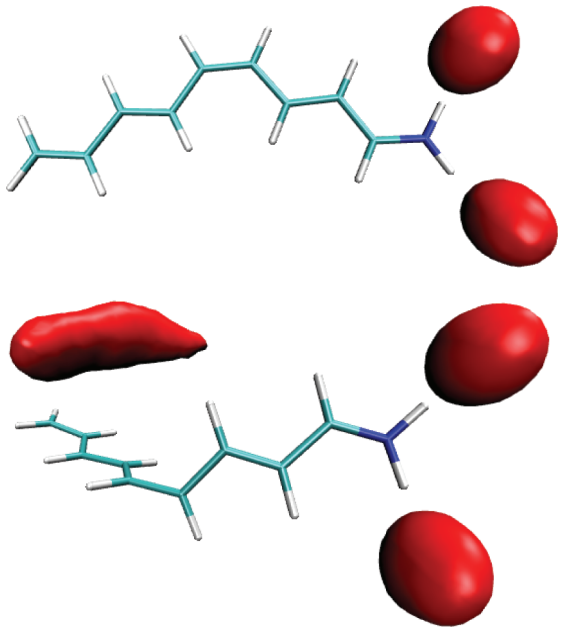

Figure 6. Occupancy maps of methanol oxygen atoms (considered as van der Waals spheres, as calculated by VMD)[52] around M1 for (a) the optimized ground-state structure and (b) the optimized EQ-MECI structure. Isosurfaces at a value of 0.77.

de-excitation times are probably associated to the solvent dynamics. As we have already indicated, during the *cis*−*trans* photoisomerization of retinal, there are parts of the solute molecule that can suffer large displacements, consequently, it can be expected that the solvent reorganization would become an important step in the nonradiative decay path. In order to clarify the role played by the solvent dynamics, we studied the evolution of the system supposing frozen solvent conditions, i.e., when the solvent is not permitted to relax after the absorption process. Under these conditions our search with the Bearpark algorithm did not locate a low-lying S_1/S_0 CI for the studied process. If the solvent is considered as fixed and in equilibrium with the charge distribution of the S_0 state, the rotation around the C_5C_6 bond during the photoisomerization process, assuming the same simple mechanism found with equilibrated solvent, implies the overlap between the solvent molecules and part of the solute. Because of this steric hindrance, a certain degree of solvent reorganization during the IC process is compulsory or the isomerization mechanism must change. This solvent reorganization is necessary also to stabilize the EQ-MECI. Figure 6 displays the occupancy maps of methanol oxygen atoms around the FC and EQ-MECI structures. At the FC point, the solvent is mainly concentrated around the iminium end that is where most of the charge is localized. In the EQ-MECI, a similar concentration of solvent molecules around the iminium is found, but there is also a high concentration around the carbon skeleton because in this case part of the charge is spread out over the whole molecule. These solvent molecules help to stabilize the charge and hence the EQ-MECI.

The question arises as to whether this difficulty in locating the CI in frozen solvent conditions is due to electrostatic or steric effects. In order to check this, we replaced the solvent representation in ASEP/MD (a set of point charges plus Lennard-Jones

parameters) by a multipole monocentric expansion, centered on the solute molecule, of the electrostatic potential, up to the hexadecapolar field. In any case, the external perturbation represents the average solvent obtained from the MD simulations of the ground state. This alternate solvent representation includes only the electrostatic contribution and discards steric effects. As a validation, the vertical absorption energy obtained with the multipole expansion was comparable to the ASEP/MD result. With this static (frozen) multipole solvent representation, we tried to locate a FS-MECI for the solute, and we could obtain it with a structure very similar to that found in the equilibrium solvent condition: a central bond length of 1.47 Å, dihedral of 90°, and BLA of 0.09 Å. Within this external perturbation, the FS-MECI is only 0.3 eV more stable than the FC point, while with ASEP/MD it is 1.58 eV lower at CASSCF level. These results point to the steric hindrance as the main reason of the loss of the CI in frozen solvent conditions and also evidence the importance that solvent relaxation has on the EQ-MECI stabilization (around 1.3 eV). Burghardt et al.,[6] in a theoretical study of a simplified model with only one double bond and using a continuum method to represent the solvent, obtained a different result; they concluded that the loss of the CI in frozen solvent conditions was due to the destabilization of the ionic state by the reaction field generated by the solvent.

Turning to the fluorescence spectra, our data indicate that the low-frequency parts of the emission band could originate from different regions of the first excited surface, S_1, of different electronic character, ionic and covalent, and we have thus a case of dual fluorescence. The high-frequency part is due to emission from the covalent minimum on S_1, while the low-frequency part is due to emission from the ionic minimum also on S_1. The relative energies of the two fluorescence maxima agree with the data reported by Zgrablić et al.[28] Given that the S_1/S_2 conical intersection is near the FC point, this double fluorescence appears mainly when the excitation energy is close or larger than the vertical excitation energy, a fact confirmed by the experiment. If the excitation energy corresponds to the 00 band (the point in which absorption and emission spectra intersect), only the ionic minimum seems to be populated.

Regarding the three decay components exhibited by the vibrationally cold S_1 fluorescence, Zgrablić et al.[28] conclude that they are due to the heterogeneity of the S_1 state in the sense that emission stems from several shallow potential surface minima. Our results have not permitted us to corroborate this conclusion. In gas phase, several ionic minima were found on S_1, however in methanol solution, we found only one minimum. This minimum is very shallow; in fact, the free energy surface is very flat in the neighborhood of this minimum. So for instance, when the minima located in gas phase, Ion-1 and Ion-2, are solvated, their free energies differ only in 1.3 and 0.4 kcal/mol, respectively, from the ionic minimum found in methanol. The different relaxation times could correspond to molecules that follow slightly different paths on this flat free energy surface. However, given the different approximations employed in our calculations, we cannot exclude the existence of multiple minima on the S_1 surface. Multiexponential decay even with a single minimum has been proposed by Olivucci and co-workers when the minimum is separated from the CI by a shallow barrier, as is the case.[53] In this proposal the different decay times are due to different amounts of kinetic energy in the reactive torsion mode. Finally, an alternative mechanism, suggested by Hasson et al.,[54] could also explain the multiexponential decay. This can arise if the solvent fluctuations modulate the barrier height leading to the reactive region on S_1. In order to check the validity of this last approximation, the energy of the ionic minimum and of the barrier for some particular solvent configurations evenly distributed along the simulation was calculated. In both cases, the fluctuation measured as the standard deviation is 0.7 kcal/mol. The height of the barrier to be surmounted to access the CI region depends on the solvent configuration considered. The solvent not only modulates the barrier height but also changes the relative stability of covalent and ionic states at different points of the free energy surface. In Figure 4, for instance, at the geometry of the ionic minimum, the covalent state is 15.7 kcal/mol above the ionic state. This value has been obtained supposing the solvent in equilibrium with the charge distribution of the ionic state. If we recalculate the energies of the two excited states at the same geometry but with the solvent now in equilibrium with the charge distribution of the covalent state, then the stability order is reversed, i.e., the covalent state becomes more stable than the ionic state. The same occurs at the geometry of the covalent minimum, where the ionic state can become more stable than the covalent when one permits the solvent to equilibrate with the ionic state. In short, as said before, fluctuations in the solvent yield to the crossing of covalent and ionic states at both minimum geometries and at the FC point. The presence of a S_1/S_2 conical intersection modulated by solvent fluctuations could permit that part of the population be transferred from the ionic to the covalent excited state and back again and that could explain the various emission times found from the ionic excited state.

Given the different approximations of our calculations, including the use of CASSCF geometries and the neglect of vibrational contributions of the solute and the importance that solvent dynamics apparently has, there is a need for much more investigation before one can elucidate which of the proposals—several minima, different amounts of kinetic energy in the reactive torsion mode, or a distribution of barrier heights modulated by the solvent—is the correct one.

4. CONCLUSIONS

We have applied the ASEP/MD method to the study of solvent effects on the radiative and nonradiative decay of a model of retinal. In particular, we have focused our study on the first step in the *cis*−*trans* photoisomerization in methanol solution. Several ionic minima that differ in less than 1 kcal/mol have been located on S_1 in gas phase, whereas in methanol only one ionic minimum has been found. On the covalent excited surface several planar minima have also been found both in gas phase and in methanol. From a photochemical point of view, the most remarkable characteristic of the ionic excited state surface is the presence of the S_0/S_1 conical intersection. The optimized CI structures are similar in vacuum and in solution, with an important torsion of ∼90° in the central double bond. In both phases, the evolution toward the conical intersection is practically a barrierless process. In gas phase, the de-excitation mainly proceeds nonradiatively through the conical intersection. In methanol solution, before the S_0/S_1 conical intersection can be reached, it needs a strong solvent reorganization, and the nonradiative route is slower; this permits the radiative decay.

We explain the structure of the emission band as a case of double fluorescence, where emission originates from two minima, ionic and covalent, on S_1. After excitation, part of the population goes to the ionic excited-state minimum, from here some molecules

can decay radiatively giving origin to the low-frequency component of the fluorescence band, and others decay nonradiatively through the S_0/S_1 CI. We assign the high-frequency component of the fluorescence band to emission from the covalent minimum on S_1. In gas phase only two states (ground and excited ionic) are involved in the photoisomerization. On the contrary, in methanol solution three states (ground, excited ionic, and excited covalent) are needed to describe the decay. Covalent and ionic states are degenerate in the neighborhood of the FC point, furthermore energy fluctuations modulated by the solvent cause the degeneration of these states at other geometries. This fact could permit the population transfer between the ionic and covalent states.

■ ASSOCIATED CONTENT

Supporting Information. MS-CASPT2 results in methanol solution together with the CASSCF and CASPT2 energies for first three singlet states, the weights of the reference zeroth-order CASSCF wave function in the CASPT2 perturbation, the mixing coefficient of the most important state in the MS-CASPT2 treatment, and finally, the off-diagonal elements in the MS-CASPT2 symmetric Hamiltonian depending on the active space and the basis set. This material is available free of charge via the Internet at http://pubs.acs.org.

■ AUTHOR INFORMATION

Corresponding Author

*E-mail: auroraml@unex.es.

Notes

The authors declare no competing financial interest.

■ ACKNOWLEDGMENT

This work was supported by the CTQ2008-06224/BQU Project from the Ministerio de Ciencia e Innovación of Spain, cofinanced by the European Regional Development Fund (ERDF), and the PRI08A056 Project from the Consejería de Economía, Comercio e Innovación of the Junta de Extremadura. I.F.G. acknowledges the Junta de Extremadura and the European Social Fund for financial support. A.M.-L. acknowledges financial support from the Juan de la Cierva subprogramme of the Ministerio de Ciencia en Innovación of Spain. The authors also thank the Fundación Computación y Tecnologías Avanzadas de Extremadura (COMPUTAEX) for additional computational resources.

■ REFERENCES

(1) Yarkony, D. R. In *Conical Intersections, Advanced Series in Physical Chemistry*; Domcke, W., Yarkony, D. R., Köppel, H., Eds.; World Scientific: Singapore, 2004; Chapter 2, No. 15, p 41.

(2) Olivucci, M.; Sinicropi, A. In *Computational Photochemistry, Theoretical and Computational Chemistry*; Olivucci, M., Ed.; Elsevier: Amsterdam, The Netherlands, 2005; Chapter I, No. 16, p 1.

(3) Yarkony, D. R. *J. Chem. Phys.* **1990**, *92*, 2457.

(4) Atchity, G. J.; Xantheas, S. S.; Ruedenberg, K. *J. Chem. Phys.* **1991**, *95*, 1862.

(5) (a) Reguero, M.; Olivucci, M.; Bernardi, F.; Robb, M. A. *J. Am. Chem. Soc.* **1994**, *116*, 2103. (b) Ragazos, N.; Robb, M. A.; Bernardi, F.; Olivucci, M. *Chem. Phys. Lett.* **1992**, *197*, 217.

(6) Burghardt, I.; Cederbaum, L.; Hynes, J. T. *Faraday Discuss.* **2004**, *127*, 395.

(7) Spezia, R.; Burghardt, I.; Hynes, J. T. *Mol. Phys.* **2006**, *104*, 903.

(8) Santoro, F.; Barone, V; Gustavsson, T.; Improta, R. *J. Am. Chem. Soc.* **2006**, *128*, 16312.

(9) Yamazaki, S.; Kato, S. *J. Chem. Phys.* **2005**, *123*, 114510.

(10) (a) Ten-no, S.; Hirata, F.; Kato, S. *J. Chem. Phys.* **1994**, *100*, 7443. (b) Sato, H.; Hirata, F.; Kato, S. *J. Chem. Phys.* **1996**, *105*, 1546.

(11) Mori, T.; Nakano, K.; Kato, S. *J. Chem. Phys.* **2010**, *133*, 064107.

(12) (a) Toniolo, A.; Granucci, G.; Martínez, T. J. *J. Phys. Chem. A* **2003**, *107*, 3822. (b) Toniolo, A.; Ben-Nun, M.; Martínez, T. J. *J. Phys. Chem. A* **2002**, *106*, 4679.

(13) Garavelli, M.; Rugen, F.; Ogliano, F.; Bearpark, M. J.; Bernardi, F.; Olivucci, M.; Robb, M. A. *J. Comput. Chem.* **2003**, *24*, 1357.

(14) Ciminelli, C.; Granucci, G.; Persico, M. *Chem.—Eur. J.* **2004**, *10*, 2327.

(15) (a) Muñoz-Losa, A.; Fdez. Galván, I.; Martín, M. E.; Aguilar, M. A. *Chem. Phys. Lett.* **2007**, *443*, 76. (b) Muñoz-Losa, A.; Fdez. Galván, I.; Sánchez, M. L.; Martín, M. E.; Aguilar, M. A. *J. Phys. Chem. B* **2008**, *112*, 877.

(16) Schoenlein, W. P.; Peteanu, L. A.; Mathies, R. A.; Shank, C. V. *Science* **1991**, *254*, 412.

(17) Wang, Q.; Schoenlein, R. W.; Peteanu, L. A.; Mathies, R. A.; Shank, C. A. *Science* **1994**, *266*, 422.

(18) (a) Garavelli, M.; Celani, P.; Bernardi, F.; Robb, M. A.; Olivucci, M. *J. Am. Chem. Soc.* **1997**, *119*, 6891. (b) Gonzalez-Luque, R.; Garavelli, M.; Bernardi, F.; Merchan, M.; Robb, M. A.; Olivucci, M. *Proc. Natl. Acad. Sci. U.S.A.* **2000**, *97*, 9379.

(19) (a) Cembran, A.; Bernardi, F.; Olivucci, M; Garavelli, M. *J. Am. Chem. Soc.* **2004**, *126*, 16018. (b) Cembran, A.; Bernardi, F.; Olivucci, M; Garavelli, M. *Proc. Natl. Acad. Sci. U.S.A.* **2005**, *102*, 6255.

(20) Coto, P. B.; Strambi, A.; Olivucci, M. *Chem. Phys.* **2008**, *347*, 483.

(21) Send, R.; Sundholm, D. *J. Phys. Chem. A* **2007**, *111*, 8766.

(22) Warshel, A.; Chu, Z. T. *J. Phys. Chem. B* **2001**, *105*, 9857.

(23) Finley, J.; Malmqvist, P-Å.; Roos, B. O.; Serrano-Andrés, L. *Chem. Phys. Lett.* **1998**, *288*, 299.

(24) Schoenlein, R. W.; Peteanu, L. A.; Mathies, R. A.; Shank, C. V. *Science* **1991**, *254*, 412.

(25) Kandori, H.; Katsuta, Y.; Ito, M.; Sasabe, H. *J. Am. Chem. Soc.* **1995**, *117*, 2669.

(26) Kandori, H.; Sasabe, H.; Nakanishi, K.; Yoshizawa, T.; Mizukami, T.; Shichida, Y. *J. Am. Chem. Soc.* **1996**, *118*, 1002.

(27) (a) Polli, D.; Altoè, P.; Weingart, O.; Spillane, K. M.; Manzoni, C; Brida, D.; Tomasello, G.; Orlandi, G; Kukura, P; Mathies, R. A.; Garavelli, M; Cerullo, G. *Nature* **2010**, *467*, 440. (b) Frutos, L. M.; Andruniów, T.; Santoro, F.; Ferré, N.; Olivucci, M. *Proc. Natl. Acad. Sci. U.S.A.* **2007**, *104*, 7764.

(28) Zgrablić, G.; Haacke, S.; Chergui, M. *J. Phys. Chem. B* **2009**, *113*, 4384.

(29) Ishida, T.; Nanbu, S.; Nakamura, H. *J. Phys. Chem. A* **2009**, *113*, 4356.

(30) (a) Fdez. Galván, I.; Sánchez, M. L.; Martín, M. E.; Olivares del Valle, F. J.; Aguilar, M. A. *Comput. Phys. Commun.* **2003**, *155*, 244. (b) Sánchez, M. L.; Martín, M. E.; Aguilar, M. A.; Olivares del Valle, F. J. *J. Comput. Chem.* **2000**, *21*, 705. (c) Martín, M. E.; Sánchez, M. L.; Olivares del Valle, F. J.; Aguilar, M. A. *J. Chem. Phys.* **2002**, *116*, 1613. (d) Sánchez, M. L.; Martín, M. E.; Fdez. Galván, I.; Olivares del Valle, F. J.; Aguilar, M. A. *J. Phys. Chem. B* **2002**, *106*, 4813.

(31) Bearpark, M. J.; Robb, M. A; Schlegel, H. B. *Chem. Phys. Lett.* **1994**, *223*, 269.

(32) (a) Chandrasekhar, J.; Smith, S. F.; Jorgensen, W. L. *J. Am. Chem. Soc.* **1985**, *107*, 154. (b) Chandrasekhar, J.; Jorgensen, W. L. *J. Am. Chem. Soc.* **1985**, *107*, 2974. (c) Jorgensen, W. L. *Acc. Chem. Res.* **1989**, *22*, 184.

(33) (a) Muñoz-Losa, A.; Fdez. Galván, I.; Martín, M. E.; Aguilar, M. A. *J. Phys. Chem. B* **2006**, *110*, 18064. (b) Muñoz-Losa, A.; Fdez. Galván, I.; Aguilar, M. A.; Martín, M. E. *J. Phys. Chem. B* **2008**, *112*, 8815.

(34) Nielsen, I. B.; Lammich, L.; Andersen, L. H. *Phys. Rev. Lett.* **2006**, *96*, 018304.
(35) Frisch, M. J.; Trucks, G. W.; Schlegel, H. B.; Scuseria, G. E.; Robb, M. A.; Cheeseman, J. R.; Zakrzewski, V. G.; Montgomery, J. A., Jr.; Stratmann, R. E.; Burant, J. C.; Dapprich, S.; Millam, J. M.; Daniels, A. D.; Kudin, K. N.; Strain, M. C.; Farkas, O.; Tomasi, J.; Barone, V.; Cossi, M.; Cammi, R.; Mennucci, B.; Pomelli, C.; Adamo, C.; Clifford, S.; Ochterski, J.; Petersson, G. A.; Ayala, P. Y.; Cui, Q.; Morokuma, K.; Malick, D. K.; Rabuck, A. D.; Raghavachari, K.; Foresman, J. B.; Cioslowski, J.; Ortiz, J. V.; Stefanov, B. B.; Liu, G.; Liashenko, A.; Piskorz, P.; Komaromi, I.; Gomperts, R.; Martin, R. L.; Fox, D. J.; Keith, T.; Al-Laham, M. A.; Peng, C. Y.; Nanayakkara, A.; Gonzalez, C.; Challacombe, M.; Gill, P. M. W.; Johnson, B. G.; Chen, W.; Wong, M. W.; Andres, J. L.; Head-Gordon, M.; Replogle, E. S.; Pople, J. A. *Gaussian 98*, revision A11.3; Gaussian, Inc.: Pittsburgh, PA, 1998.
(36) Refson, K. *Comput. Phys. Commun.* **2000**, *126*, 310.
(37) Karlström, G.; Lindh, R.; Malmqvist, P.-Å.; Roos, B. O.; Ryde, U.; Veryazov, V.; Widmark, P.-O.; Cossi, M.; Schimmelpfennig, B.; Neogrády, P.; Seijo, L. *Comput. Mater. Sci.* **2003**, 28222.
(38) Ghigo, G.; Roos, B. O.; Malmqvist, P-Å. *Chem. Phys. Lett.* **2004**, *396*, 142.
(39) Cornell, W. D.; Cieplack, P.; Bayly, C. I.; Groud, K. M.; Ferguson, D. M.; Spellmeyer, D. C.; Fox, T.; Cladwell, J. W.; Kollman, P. A. *J. Am. Chem. Soc.* **1995**, *117*, 5179.
(40) Rajamani, R.; Gao, J. *J. Comput. Chem.* **2002**, *23*, 96.
(41) Röhrig, U. F.; Guidoni, L.; Rothlisberger, U. *ChemPhysChem* **2005**, *6*, 1836.
(42) Platz, P. E.; Moheler, J. H. *Biochemistry* **1975**, *14*, 2340.
(43) Levine, B. G.; Martinez, T. J. *Annu. Rev. Phys. Chem.* **2007**, *58*, 613.
(44) Valsson, O.; Filippi, C. *J. Chem. Theory Comput.* **2010**, *6*, 1275.
(45) Garavelli, M.; Vreven, T.; Celani, P.; Bernardi, F.; Robb, M. A.; Olivucci, M. *J. Am. Chem. Soc.* **1998**, *120*, 1285.
(46) Warshel, A. *Nature* **1976**, *260*, 679.
(47) Schapiro, I.; Weingart, O.; Buss, V. *J. Am. Chem. Soc.* **2009**, *131*, 16.
(48) Rostov, I. V.; Amos, R. D.; Kobayashi, R.; Scalmani, G.; Frisch, M. J. *J. Phys. Chem. B* **2010**, *114*, 5547.
(49) Kochendoerfer, G. G.; Mathies, R. A. *J. Phys. Chem.* **1996**, *100*, 14526.
(50) Fdez. Galván, I.; Sánchez, M. L.; Martín, M. E.; Olivares del Valle, F. J.; Aguilar, M. A. *J. Chem. Phys.* **2003**, *118*, 255.
(51) Serrano-Andrés, L.; Merchán, M.; Lindh, R. *J. Chem. Phys.* **2005**, *122*, 104107.
(52) Humphrey, W.; Dalke, A.; Schulten, K. *J. Mol. Graphics* **1996**, *14*, 33.
(53) Olivucci, M.; Lami, A.; Santoro, F. *Angew. Chem., Int. Ed.* **2005**, *44*, 5118.
(54) Hasson, K. C.; Gai, F.; Anfinrud, P. A. *Proc. Natl. Acad. Sci. U.S.A.* **1996**, *93*, 15124.